

Article

Not peer-reviewed version

Screening of a 4-Ethylguaiacol-Producing *Bacillus coagulans* JN11 and Characterization of Its Phenolic Acid Decarboxylase BcPAD

[Yufeng Liu](#) , Hao Wang , Xinyue Lan , Rui Wang , Can Liu , [Jun Liu](#) , [He Zou](#) , [Siqi Yuan](#) *

Posted Date: 29 April 2026

doi: 10.20944/preprints202604.2010.v1

Keywords: 4-ethylguaiacol; *Bacillus coagulans*; phenolic acid decarboxylase; enzymatic characterization; substrate specificity; molecular docking



Preprints.org is a free multidisciplinary platform providing preprint service that is dedicated to making early versions of research outputs permanently available and citable. Preprints posted at Preprints.org appear in Web of Science, Crossref, Google Scholar, Scilit, Europe PMC, OpenAlex.

Copyright: This open access article is published under a [Creative Commons CC BY 4.0 license](#), which permit the free download, distribution, and reuse, provided that the author and preprint are cited in any reuse.

Disclaimer/Publisher's Note: The statements, opinions, and data contained in all publications are solely those of the individual author(s) and contributor(s) and not of MDPI and/or the editor(s). MDPI and/or the editor(s) disclaim responsibility for any injury to people or property resulting from any ideas, methods, instructions, or products referred to in the content.

Article

Screening of a 4-Ethylguaiacol-Producing *Bacillus coagulans* JN11 and Characterization of Its Phenolic Acid Decarboxylase BcPAD

Yufeng Liu ^{1,2}, Hao Wang ¹, Xinyue Lan ¹, Rui Wang ¹, Can Liu ¹, Jun Liu ^{1,2}, He Zou ^{1,2} and Siqi Yuan ^{1,2,*}

¹ School of Food and Liquor Engineering, Sichuan University of Science & Engineering, Yibin 644000, China

² Brewing Science and Technology Key Laboratory of Sichuan Province, Sichuan University of Science & Engineering, Yibin 644000, China

* Correspondence: yuansiqi@suse.edu.cn

Abstract

4-Ethylguaiacol (4-EG) is an important volatile phenolic compound that contributes characteristic smoky, woody, and spicy notes to fermented foods and beverages, particularly Baijiu. In this study, a 4-EG-producing strain, designated JN11, was obtained by screening isolates from Baijiu pit mud and identified as *Bacillus coagulans* based on morphological, physiological, biochemical, and 16S rRNA analyses. In sorghum juice medium, strain JN11 produced 271.57 ± 2.73 $\mu\text{g/L}$ 4-EG. To elucidate its role in volatile phenol formation, the phenolic acid decarboxylase gene, *BcPAD*, was cloned and heterologously expressed in *Escherichia coli* BL21(DE3). The *BcPAD* gene comprises 504 bp and encodes a 167-amino-acid protein. Recombinant BcPAD exhibited maximal activity at pH 6.0 and 50 °C and retained more than 60% residual activity after 5 h at 30–40 °C. Fe³⁺ increased enzyme activity to 115.36% of the control, whereas Zn²⁺ markedly inhibited enzyme activity and SDS completely inactivated the enzyme. BcPAD showed the highest activity toward *p*-coumaric acid, with a specific activity of 460.55 ± 18.30 U/mg and a catalytic efficiency (K_{cat}/K_m) of 6.26 ± 0.75 $\text{mM}^{-1} \cdot \text{s}^{-1}$, while lower activities were observed toward caffeic acid and ferulic acid, and no activity was detected toward sinapic acid. Homology modeling and molecular docking further indicated that the superior catalytic performance toward *p*-coumaric acid was associated with favorable hydrogen-bonding interactions and a productive binding orientation within the active site. These findings provide new insights into phenolic acid decarboxylases from *B. coagulans* and support the potential applications of strain JN11 and BcPAD in volatile phenol biosynthesis and flavor modulation during Baijiu production.

Keywords: 4-ethylguaiacol; *Bacillus coagulans*; phenolic acid decarboxylase; enzymatic characterization; substrate specificity; molecular docking

1. Introduction

4-Ethylguaiacol (4-EG) is an important volatile phenolic flavor compound with characteristic smoky, woody, spicy, and slightly sweet notes [1] and is widely found in fermented foods such as Baijiu, soy sauce, and pickles [2]. In Chinese Baijiu, 4-EG is considered one of the key trace aroma-active compounds contributing to the Jiang-flavor style, and at appropriate concentrations, it enhances the mellow mouthfeel of the liquor [3]. In addition to its sensory contribution, 4-EG also exhibits notable reactive oxygen species scavenging capacity and anti-inflammatory effects, showing potential physiological activities in aspects such as antioxidation, cardiovascular disease prevention, and the treatment of central nervous system disorders [4–6]. Therefore, 4-EG is not only an important flavor compound in Baijiu but also a potential health-related factor, and has been widely applied in industries such as alcoholic beverages, soy sauce, and tobacco [3,7]. Currently, the main approaches

for 4-EG production include natural extraction, chemical synthesis, and biotransformation [8]. Compared with natural extraction, which is limited by low extraction efficiency and restricted raw material availability, and chemical synthesis, which involves harsh reaction conditions and greater environmental burdens, biotransformation has attracted widespread attention because of its mild conditions, high selectivity, and environmental friendliness [9].

Phenolic acids mainly include hydroxycinnamic acid compounds such as ferulic acid, *p*-coumaric acid, caffeic acid, and sinapic acid [10]. These compounds are widely present in plant cell walls and agro-industrial by-products, usually in free or bound forms, and can be released by the action of esterases or other lignocellulose-degrading enzymes [11]. Phenolic acid decarboxylase (PAD, EC 4.1.1.102) catalyzes the non-oxidative decarboxylation of these hydroxycinnamic acids to produce 4-vinyl derivatives [12], including 4-vinylguaiacol (4-VG), which are generally of high economic value [13]. Among these products, 4-VG can be further converted into 4-EG by reductases [10]. Therefore, as a key enzyme in the biosynthetic pathway of 4-EG, PAD-based biotransformation strategies show promising prospects for the sustainable production of natural flavor compounds and the valorization of agro-industrial residues. Previous studies have shown that PAD is mainly found in bacteria, fungi, and a few plants [14]. PADs from different sources exhibit significant differences in enzymatic and biochemical properties. For example, the optimal pH of dLPPAD from *Pichia pastoris* is 7.0 [12], whereas the optimal pH of FADase from *Enterobacter* sp. Px6-4 is 4.0 [15]. In addition, BsPAD from *Bacillus subtilis* exhibits an optimal reaction temperature of 50 °C [16], whereas CgPAD from *Candida guilliermondii* exhibits maximal activity at 25 °C [17]. Overall, bacterial PADs generally display high catalytic activity, while PADs from *Bacillus* species possess advantages in thermal stability and environmental tolerance [14], highlighting their considerable potential in flavor biomanufacturing and enzyme engineering. In recent years, related studies have gradually expanded from strain screening to gene cloning, heterologous expression, enzymatic characterization, and catalytic mechanism analysis [12,18,19]. However, current research has mainly focused on lactic acid bacteria, yeasts, and a few model strains, and systematic studies on 4-EG-producing functional microorganisms and their key enzyme, PAD, in the Baijiu fermentation system remain limited. In particular, in-depth studies on the molecular characteristics, enzymatic properties, and substrate recognition mechanism of PAD derived from *B. coagulans* are still lacking.

Daqu (fermentation starter) and pit mud are complex microbial ecosystems enriched in functional microorganisms closely associated with flavor formation [20]. Among these microorganisms, members of the genus *Bacillus* are regarded as important aroma-producing microbes during Baijiu fermentation due to their high heat resistance, strong environmental adaptability, and considerable metabolic diversity [21]. However, despite increasing interest in volatile phenol biosynthesis, systematic studies on 4-EG-producing functional microorganisms and their key phenolic acid decarboxylases in the Baijiu fermentation system remain limited, particularly with respect to *B. coagulans*. Therefore, in the present study, *Bacillus* strains were isolated and screened from *Daqu* and pit mud, and a 4-EG-producing strain, designated JN11, was identified as *B. coagulans*. Subsequently, its growth characteristics and environmental tolerance were analyzed, its phenolic acid decarboxylase gene *BcPAD* was cloned and heterologously expressed, and the enzymatic properties, substrate specificity, and kinetic parameters of recombinant BcPAD were systematically investigated. In addition, the structural basis for substrate recognition was analyzed using homology modeling and molecular docking. This study provides mechanistic insights into volatile phenol formation by *B. coagulans* and offers a theoretical basis for the potential applications of strain JN11 and BcPAD in the biosynthesis of volatile phenolic compounds and flavor modulation during Baijiu production.

2. Materials and Methods

2.1. Strains, Plasmids and Chemicals

Information on the nine bacterial strains and three plasmids used in this study is presented in Table 1. The bacterial genomic DNA extraction kit was purchased from Labgic Technology Co., Ltd. (Beijing, China). DNA polymerase, T4 DNA ligase, BamH I and Hind III restriction endonucleases, and DNA and protein molecular weight markers were purchased from TransGen Biotech Co., Ltd. (Beijing, China). Kanamycin (Kan) and isopropyl- β -D-thiogalactopyranoside (IPTG) were purchased from Solarbio Science & Technology Co., Ltd. (Beijing, China). pentyl acetate, ethylene diamine tetraacetic acid (EDTA), sodium dodecyl sulfate (SDS), 4-ethylguaiacol, ferulic acid (FA), *p*-coumaric acid (PCA), caffeic acid (CA), and sinapic acid (SA) were purchased from Yuanye Biotechnology Co., Ltd. (Shanghai, China).

Table 1. Strains and plasmids used in this study.

Strains/plasmids	Description	Source
JXQ2	The strain was isolated from the high-temperature <i>Daqu</i>	Lab stock
JXQ5	The strain was isolated from the high-temperature <i>Daqu</i>	Lab stock
NXQ4	The strain was isolated from the medium-temperature <i>Daqu</i>	Lab stock
JN2	The strain was isolated from the mud of the liquor cellar	Lab stock
JN11	The strain was isolated from the mud of the liquor cellar	Lab stock
<i>E. coli</i> BL21(DE3)	Host for gene expression	TransGen
<i>E. coli</i> BL21(DE3)/pET-28a	Expression strain carrying plasmid pET-28a	This work
<i>E. coli</i> BL21(DE3)/pET-28a- <i>BcPAD</i>	Expression strain carrying plasmid pET-28a- <i>BcPAD</i>	This work
pET-28a(+)	<i>E. coli</i> expression vector, Kan ^r	TaKaRa
pET-28a- <i>BcPAD</i>	pET-28a(+) derivative harboring <i>BcPAD</i> gene, Kan ^r	This work

2.2. Screening of 4-EG-Producing Strains

Bacillus strains (JXQ2, JXQ5, NXQ4, JN2, and JN11) stored at -80 °C were individually streaked onto de Man, Rogosa and Sharpe (MRS) agar plates and incubated at 37 °C for 16 h to reactivate the cultures. Single colonies were then selected and inoculated into LB broth and cultured at 37 °C with shaking at 180 rpm for 16 h. Subsequently, the seed cultures at an inoculum size of 1×10^6 CFU/mL were inoculated into the sorghum juice fermentation medium [22,23]. After 7 d of fermentation, the volatile compounds and 4-EG concentration in the fermentation products were analyzed using gas chromatography-mass spectrometry (GC-MS), and the strain exhibiting the highest 4-EG production was selected for subsequent experiments.

The fermentation broth was centrifuged at 8000 rpm for 5 min, and the resulting supernatant was filtered through a 0.22 μ m membrane filter. Then, 1 mL of the filtrate was transferred into a 15 mL headspace bottle, and 20 μ L of the internal standard solution (10 g/L pentyl acetate) was added. The sample was heated in a 60 °C metal bath for 15 min, after which the extraction fiber was inserted into the headspace bottle for adsorption extraction for 45 min. After extraction, the volatile compounds were analyzed by GC-MS. GC conditions were as follows: a DB-WAX capillary column (30 m \times 0.25 mm, 0.25 μ m) was used for manual injection, and the injector temperature was maintained at 230 °C. The oven temperature program was as follows: the initial temperature was set at 65 °C and held for 3 min, then increased to 150 °C at a rate of 5 °C/min and held for 2 min, followed

by a further increase to 230 °C at 10 °C/min, where it was maintained for 10 min. Helium was used as the carrier gas at a flow rate of 0.8 mL/min, with a split ratio of 20 : 1 and an injection volume of 1 µL. MS conditions were as follows: electron ionization was employed, the mass scan range was m/z 20–500, the electron energy was 70 eV, the ion source temperature was 230 °C, the quadrupole temperature was 150 °C, and the solvent delay time was 3 min.

2.3. Identification and Physiological Characterization of the 4-EG-Producing Strain

Strain identification was based on colony morphology, biochemical characteristics, and molecular phylogenetic analysis. Morphological observation and biochemical characterization of the strain were conducted according to Bergey's Manual of Determinative Bacteriology [24]. Molecular phylogenetic analysis was performed according to a previously reported method [25]. Genomic DNA was extracted from the strain using a bacterial genomic DNA extraction kit, and the 16S rRNA gene was amplified using the primers 27F (5'-AGAGTTTGATCCTGGCTCAG-3') and 1492R (5'-GGTTACCTTGTTACGACTT-3'). The PCR products were examined by 1% (w/v) agarose gel electrophoresis and then sent to Youkang Biotechnology Co., Ltd. (Chengdu, China) for sequencing. The obtained sequences were subjected to BLAST homology analysis, and a phylogenetic tree was constructed using the neighbor-joining method in MEGA 6.0 software with 1,000 random bootstrap replications.

To determine the growth curve of the strain, the activated culture was inoculated into MRS broth at 1% (v/v) and incubated at 37 °C with shaking at 180 rpm. The optical density (OD) 600 of the culture was measured hourly for 36 h, with uninoculated MRS broth used as the blank control. To evaluate strain tolerance under different environmental conditions, the activated culture was inoculated into MRS broth at 1% (v/v) and incubated with shaking at 180 rpm for 12 h under different pH values (4, 5, 6, 7, 8, and 9), temperatures (20, 25, 30, 35, 40, and 45 °C), ethanol concentrations (0, 2, 4, 6, 8, and 10%, v/v), sodium chloride concentrations (0, 2, 4, 6, 8, and 10%, w/v), and glucose concentrations (0, 5, 10, 15, 20, and 25%, w/v). The OD₆₀₀ was then measured. All experiments were performed in triplicate.

2.4. Cloning and Sequence Analysis of the BcPAD Gene

Based on the sequence information for the phenolic acid decarboxylase gene of *Bacillus coagulans* available in the NCBI database (GenBank accession number: WP_263931213.1), full-length amplification primers were designed: BcPAD-BamHI-F (5'-CGGGATCCATGAAAACATTAGAAGAA-3') and BcPAD-HindIII-R (5'-CCCAAGCTTTTATGAAAATTTAGTTTGAA-3'). PCR amplification was performed using the genomic DNA of *Bacillus coagulans* JN11 as the template under the following conditions: pre-denaturation at 95 °C for 4 min; 34 cycles of denaturation at 95 °C for 40 s, annealing at 55 °C for 40 s, and extension at 72 °C for 1 min; followed by a final extension at 72 °C for 10 min. The amplified product was verified by 1% (w/v) agarose gel electrophoresis and then purified. The purified target fragment and the pET-28a vector were double-digested with BamHI and HindIII, respectively. After purification of the digested products, ligation was performed using T4 DNA ligase at 25 °C for 4 h. The ligation product was transformed into *E. coli* BL21(DE3) cells, and positive colonies identified by colony PCR were sent to Youkang Biotechnology Co., Ltd. (Chengdu, China) for sequencing. Following BLAST analysis of the sequencing results, the amino acid sequence was deduced using DNAMAN software. The basic physicochemical properties of the deduced amino acid sequence were analyzed using the ProtParam tool (<https://web.expasy.org/protparam/>), and multiple sequence alignment was performed using Clustal software and ESPript 3.2 (<https://espript.ibcp.fr/ESPript/cgi-bin/ESPript.cgi>)

2.5. Heterologous Expression and Purification of Recombinant BcPAD

A single colony of the recombinant *E. coli* BL21(DE3)/pET-28a-BcPAD strain was picked and inoculated into Luria-Bertan (LB) medium containing 50 µg/mL kanamycin, followed by cultivation at 37 °C and 180 rpm for 12 h. The seed culture was then inoculated at 1% (v/v) into 100 mL of LB medium containing 50 µg/mL kanamycin and incubated at 37 °C and 180 rpm until the OD₆₀₀ reached 0.6–0.8. IPTG was added to final concentrations of 0.0, 0.1, 0.3, 0.5, 0.7, and 1.0 mmol/L, and protein expression was induced for 3 h at 180 rpm to determine the optimal IPTG concentration. Cells were collected by centrifugation at 8,000 rpm for 5 min, and protein expression levels were evaluated by sodium dodecyl sulfate-polyacrylamide gel electrophoresis (SDS-PAGE). In addition, under the optimal IPTG concentration, protein expression was induced for 16 h at different temperatures (25, 30, and 37 °C) at 180 rpm to identify the optimal temperature for soluble protein expression. Cells were harvested by centrifugation at 8,000 rpm for 5 min at 4 °C and resuspended in 10 mL of 50 mmol/L sodium phosphate buffer (Na₂HPO₄–NaH₂PO₄, pH 7.0). The cells were disrupted by ultrasonication (180 W; 3 s on, 3 s off) for 15 min in an ice bath. The supernatant was collected by centrifugation at 10,000 rpm for 5 min at 4 °C. The sediment was treated with 8 mol/L urea at 4 °C for 30 min. The distribution of the target protein in the supernatant and sediment was analyzed by SDS-PAGE. The supernatant was further purified by Ni-NTA affinity chromatography, and the target protein was eluted with 100 mmol/L imidazole. The purified protein was analyzed by SDS-PAGE and subsequently used for enzyme activity assays. The concentration of the purified protein was determined using the Bradford method [26].

2.6. Determination of Recombinant BcPAD Enzyme Activity

The standard reaction mixture consisted of 0.8 mL of Na₂HPO₄–citrate buffer (pH 6.0), 0.1 mL of 50 mmol/L FA, and 0.1 mL of 0.1354 mg/mL purified BcPAD. After incubation in a 37 °C water bath for 5 min, the reaction was terminated by the addition of 2 mL of methanol. The resulting mixture was filtered through a 0.22 µm membrane filter, and the concentration of 4-vinyl derivatives was determined by high-performance liquid chromatography (HPLC). The control was prepared by replacing the enzyme solution with 0.1 mL of Na₂HPO₄–citrate buffer. The HPLC conditions were as follows: a Potensil-C18 column (4.6 mm × 150 mm, 5 µm, Anjie, Chengdu, China), an injection volume of 5 µL, a flow rate of 1.0 mL/min, a column temperature of 30 °C, a mobile phase of methanol/0.1% acetic acid (40 : 60, v/v), and a detection wavelength of 260 nm. One unit of enzyme activity (U) was defined as the amount of enzyme required to produce 1 µmol of 4-vinyl derivative per minute.

2.7. Effects of pH, Temperature, Metal Ions, and Chemical Reagents on the Activity of BcPAD

The optimal pH of the enzyme was determined over a pH range of 5.0–8.0 using Na₂HPO₄–citrate buffer under the standard assay conditions described above. At the optimal pH, the optimal temperature of the enzyme was determined over a range of 20–70 °C. The maximum enzyme activity was defined as 100%, and the relative activity under each condition was calculated accordingly.

pH stability was evaluated by measuring residual activity after incubating the enzyme without substrate in Na₂HPO₄–citrate buffer at pH 5.0–8.0 at room temperature for 0–5 h. Thermal stability was evaluated by measuring the residual activity after incubating the enzyme in Na₂HPO₄–citrate buffer (pH 6.0) at 20–70 °C for 0–5 h. Under the same pH or temperature conditions, the activity of the non-incubated enzyme was defined as 100%, and the relative activity at different incubation times was calculated accordingly.

Under the optimal assay conditions, various metal ions (Ba²⁺, Ca²⁺, Co²⁺, Cs⁺, Cu²⁺, Fe³⁺, Li⁺, Mg²⁺, Mn²⁺, Ni²⁺, and Zn²⁺) and chemical reagents (EDTA, SDS, and urea) were individually added to the reaction mixture at a final concentration of 1 mmol/L, whereas Triton X-100 and ethanol were added at a final volume fraction of 1% to evaluate their effects on the enzyme activity. The reaction mixture without added metal ions or chemical reagents served as the control, and its enzyme activity was defined as 100%, relative to which all other activities were calculated.

2.8. Substrate Specificity and Kinetic Parameters of BcPAD

Using 80 mmol/L FA, PCA, CA, or SA as the substrate under the optimal reaction conditions, the catalytic activity of BcPAD toward each substrate was determined, and the specific activity was calculated. Kinetic analysis was performed under the optimal reaction conditions for 5 min in Na_2HPO_4 -citrate buffer containing varying concentrations (5–160 mmol/L) of FA, PCA, or CA. Nonlinear regression was performed by fitting the data to the Michaelis–Menten equation using GraphPad Prism software, and the Michaelis constant (K_m), Maximum velocity (V_{max}), Catalytic Constant (K_{cat}), and K_{cat}/K_m values for BcPAD with each substrate were calculated, respectively.

2.9. Structural Analysis of BcPAD

The crystal structure of FADase from *Lactobacillus plantarum* (PDB ID: 2W2A) was selected as the template for homology modeling of BcPAD in SWISS-MODEL (<https://swissmodel.expasy.org/>) based on amino acid sequence alignment. The structural information for the ligands FA, PCA, and CA was obtained from the PubChem database (<https://pubchem.ncbi.nlm.nih.gov/>). AutoDock Tools was used to remove water molecules and metal ions and to add hydrogen atoms. Molecular docking was performed using Autodock Vina software, with the grid box dimensions set to $39 \times 36 \times 36$ and the center coordinates set to $x = 2.252$, $y = 30.032$, and $z = 25.138$. The docking results were evaluated based on binding energy and interaction patterns, and the conformation with the lowest binding energy was selected as the final docking result. PyMOL 2.5 software was used for three-dimensional visualization of the tertiary structure and molecular docking results, and Discovery Studio 2025 software was used for two-dimensional visualization of protein–ligand interactions.

2.10. Statistical Analysis

Data are presented as the mean \pm standard error (SE) from three independent experiments. Differences among samples were analyzed using one-way analysis of variance (ANOVA) followed by Duncan's multiple range test in SPSS 27 software. Differences were considered significant at $p < 0.05$. Data were visualized using Origin 2024 software.

3. Results and Discussion

3.1. Screening and Analysis of 4-EG-Producing Strains

Using 4-EG yield as the screening indicator, GC-MS analysis showed that all five strains produced 4-EG during fermentation in sorghum juice medium (Figure 1A). The fermentation product of the JN11 strain exhibited a retention time of 33.091 min for 4-EG (Figure 1B), achieving the highest yield among all strains at $271.57 \pm 2.73 \mu\text{g/L}$. This yield surpasses the $245.30 \mu\text{g/L}$ obtained by *Bacillus cereus* wsp-2-2 utilizing wheat bran as a substrate [3], but is lower than the $460.00 \mu\text{g/L}$ obtained from *Saccharomyces fibuligera* B0 using malt juice as a fermentation medium [27]. The observed difference in yield may be attributed to the varying synthesis capabilities of the strains for 4-EG, as well as the differences in the fermentation media employed. Notably, it has been confirmed that specific strains of *Bacillus licheniformis* [28] and *Bacillus subtilis* [29] lack the capability to synthesize 4-EG. Based on the 4-EG production capabilities of the aforementioned strains, the JN11 strain was ultimately chosen for further identification, biological characterization, and functional studies on phenolic acid decarboxylase.

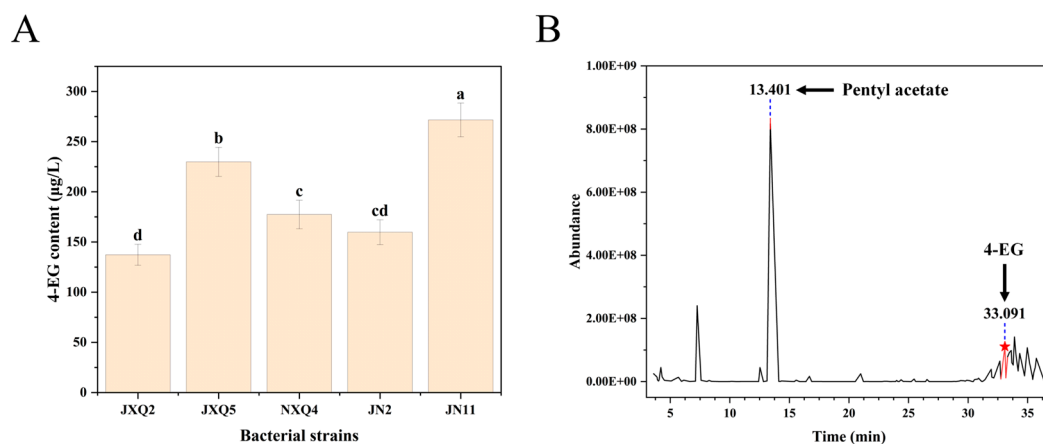


Figure 1. Analysis of 4-EG production by strains. (A) 4-EG production by different strains after 7 d of fermentation. (B) GC-MS chromatogram of the JN11 strain After 7 d of fermentation.

3.2. Identification of JN11 Strain

The JN11 strain was inoculated onto MRS medium to examine the morphology of a single colony (Figure 2A). It was observed that the colony exhibited a circular shape, a moist surface, slight elevation, and an opaque milky-white color. Following Gram staining, microscopic examination revealed that the JN11 strain appeared blue-violet, indicating that it is a Gram-positive bacterium with a relatively short rod-shaped morphology and rounded ends (Figure 2B). The biochemical characteristics of the JN11 strain are detailed in Table 2. The JN11 strain can ferment glucose, sucrose, and lactose, except for mannitol. Additionally, it exhibits activities of catalase, cellulase, and protease. The strain was positive in gelatin and starch hydrolysis, nitrate reduction, VP test, and anaerobic growth test, but negative in citrate utilization and indole test. The 16S rRNA gene of the JN11 strain was amplified by PCR (Figure 2C) and then sequenced, and the results indicated that the sequence similarity between the JN11 strain and *B. coagulans* reached 99.44%. The phylogenetic analysis further indicated that the genetic distance between the JN11 strain and *B. coagulans* K6 was the closest (Figure 2D), so it was designated as *B. coagulans* JN11.

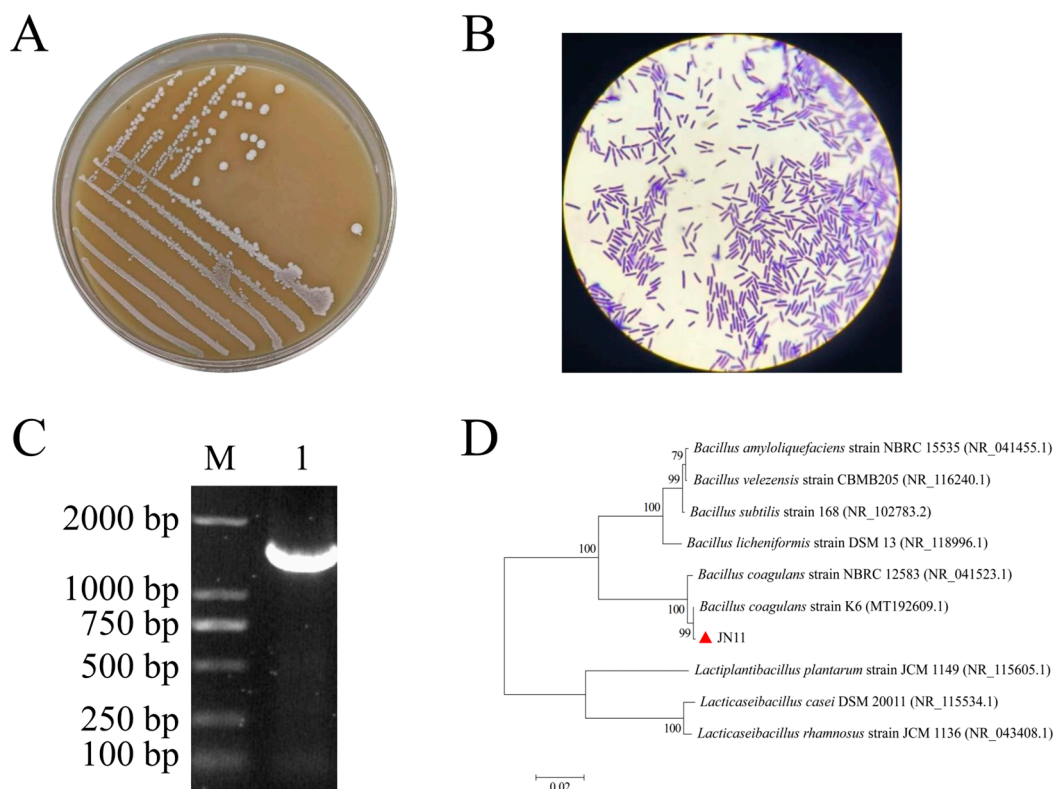


Figure 2. The morphological and genetic characteristics of the JN11 strain. (A) The morphology of the JN11 strain on MRS medium. (B) The Gram staining result of the JN11 strain (1000 ×). (C) PCR amplification product of the 16S rRNA gene from the JN11 strain. (D) The phylogenetic tree of the JN11 strain.

Table 2. Physiochemical characteristics of the JN11 strain.

Biochemical Test	Test Result	Biochemical Test	Test Result
Glucose fermentation	+	Gelatin hydrolysis	+
Sucrose fermentation	+	Starch hydrolysis	+
Lactose fermentation	+	Nitrate reduction	+
Mannitol fermentation	−	Citrate utilization	−
Catalase activity	+	VP test	+
Cellulase activity	+	Indole test	−
Proteinase activity	+	Anaerobic growth	+

+ indicates positive, − indicates negative.

3.3. Physiological Characteristics of *Bacillus Coagulans* JN11

Growth characterization experiments indicated that *B. coagulans* JN11 remained in the lag phase from 0 to 7 h, entered the logarithmic phase between 8 and 15 h, transitioned into the stationary phase from 16 to 25 h, and subsequently entered the decline phase after 25 h (Figure 3A). The strain grew over a pH range of 5 to 9, with an optimal pH of 6.0 (Figure 3B). *B. coagulans* JN11 grew over a temperature range of 20–45 °C, with the optimal growth temperature being 35 °C (Figure 3C). At ethanol volume fractions of 2–10%, growth was significantly inhibited, and when the ethanol volume fraction exceeded 8%, the strain almost ceased to grow (Figure 3D). When the NaCl concentration reached 4%, the OD of *B. coagulans* JN11 was only 26.44% of that of the control (Figure 3E). Notably, the addition of 5% glucose further stimulated growth, increasing the OD by 11.75% (Figure 3F). However, when the glucose concentration exceeded 15%, the growth of strain JN11 was significantly inhibited, although its relative OD still remained at 75.19%. In summary, *B. coagulans* JN11 prefers a mildly acidic, low-sugar environment and exhibits a certain tolerance to high temperature and ethanol, but is intolerant of high-salt conditions.

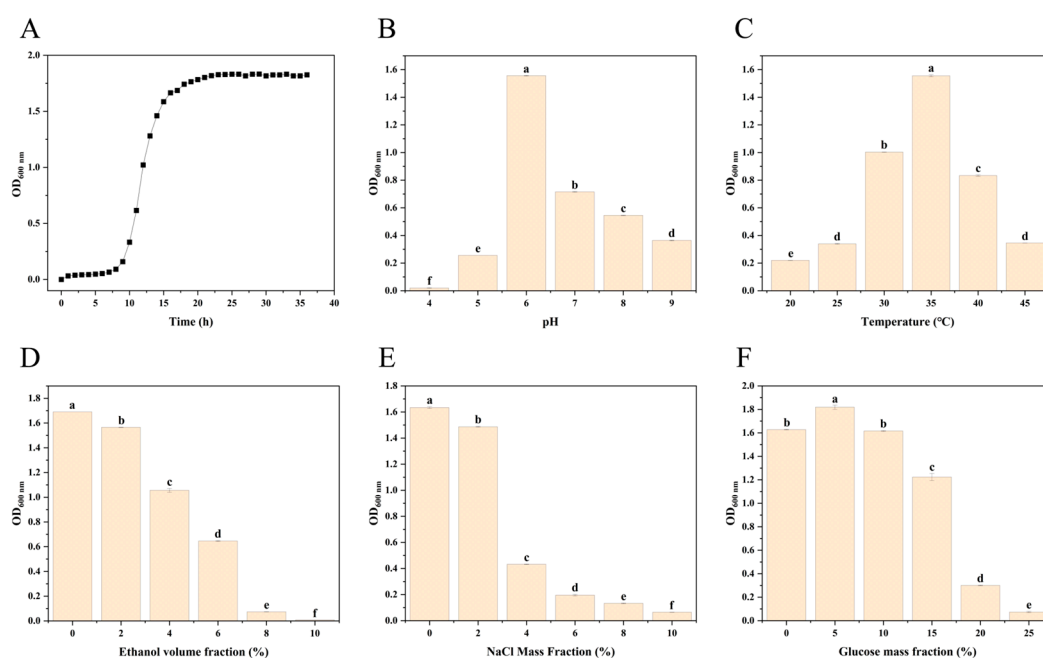


Figure 3. Growth characteristics of *B. coagulans* JN11 under different conditions. (A) Growth curve of *B. coagulans* JN11. (B) Effect of pH on the growth of *B. coagulans* JN11. (C) Effect of temperature on the growth of *B. coagulans*

JN11. (D) Effect of ethanol on the growth of *B. coagulans* JN11. (E) Effect of NaCl on the growth of *B. coagulans* JN11. (F) Effect of glucose on the growth of *B. coagulans* JN11.

3.4. Gene Cloning and Bioinformatics Analysis of BcPAD

Amplification was conducted using DNA from *B. coagulans* JN11 as a template, with primers BcPAD-BamHI-F and BcPAD-HindIII-R, resulting in the detection of a band approximately 500 bp in size through agarose gel electrophoresis (Figure 4A). Sequencing and comparative analyses confirmed that the full-length sequence of the *BcPAD* gene is 504 bp, comprising a complete open reading frame encoding 167 amino acids (Figure S1), which is similar in size to the 166 amino acids encoded by BIPAD from *Bacillus licheniformis* [30]. PCR identification was performed on transformed *E. coli* BL21(DE3) colonies harboring the pET28a-*BcPAD* ligation product. The results revealed four bands that corresponded to the expected size (Figure 4B), indicating the presence of positive clones. Sequencing of the positive clones indicated successful insertion of the *BcPAD* gene into the correct position of the pET28a vector, demonstrating that the *E. coli* BL21(DE3)-pET28a-*BcPAD* recombinant strain was constructed successfully. ProtParam analysis indicated that the theoretical isoelectric point (pI) of BcPAD is 4.93, with an associated molecular weight of 19.63 kDa. The instability index (II) was calculated to be 27.83, and the grand average of hydropathicity (GRAVY) was -0.564, indicating that the protein is both hydrophilic and stable.

An amino acid sequence alignment of BcPAD with other reported phenolic acid decarboxylases revealed that BcPAD shares the highest sequence identity of 79.50% with BsPAD from *Bacillus subtilis* (PDB ID: 4ALB) [31]. Additionally, BcPAD displays sequence identities of 77.78% with BaPAD from *Bacillus atrophaeus* (GenBank accession number: AKL86192.1) [32], 77.50% with BpPAD from *Bacillus pumilus* (PDB ID: 3NAD) [33], 72.56% with LpPDC from *Lactobacillus plantarum* (PDB ID: 2W2A) [34], and 69.94% with LvPAD from *Lactobacillus vermolensis* (GenBank accession number: WIW58156.1) [2]. Notably, the twelve key active sites of phenolic acid decarboxylases, as previously reported [18,35], are highly conserved among these enzymes (Figure 4C). These results suggest that BcPAD is a member of the phenolic acid decarboxylase family and may exhibit similar catalytic functions.

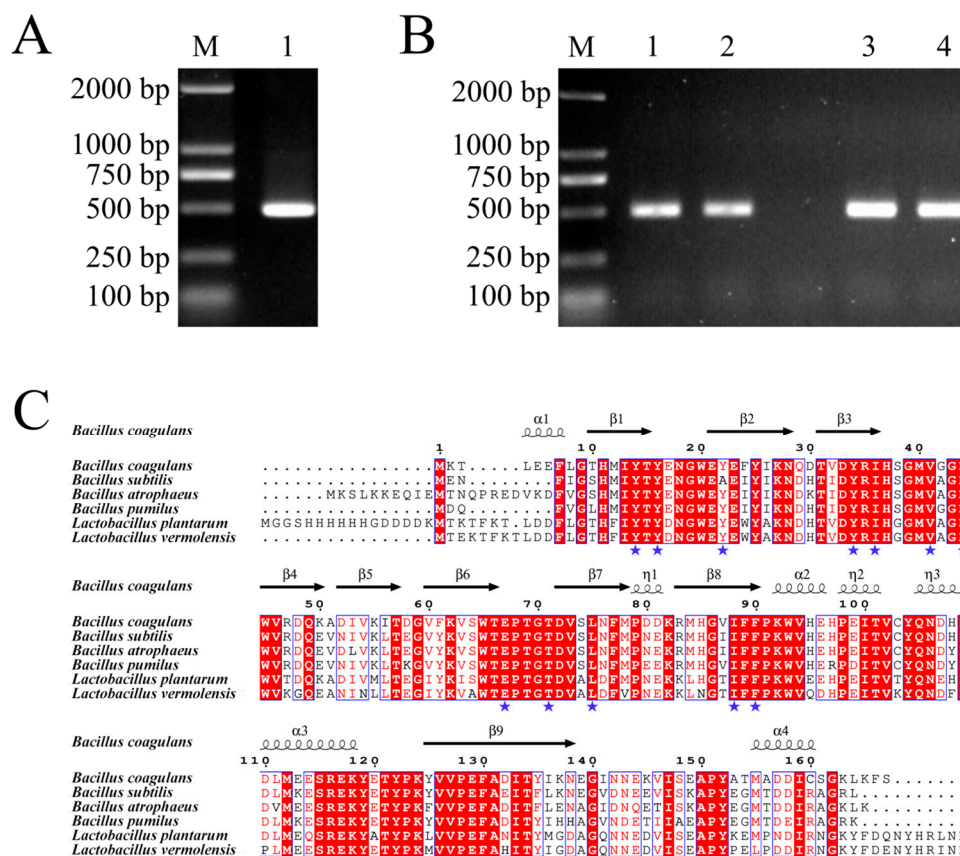


Figure 4. Gene cloning and multiple sequence alignment analysis of BcPAD. (A) PCR amplification of the *BcPAD* gene. M: DNA DL2000 Marker; Lane 1: PCR amplification product. (B) PCR identification of colonies from *E. coli* BL21(DE3)-pET28a-*BcPAD*. M: DNA DL2000 Marker; Lanes 1-4: Colony PCR products. (C) Sequence alignment of BcPAD with other identified phenolic acid decarboxylase. Consistent amino acid sequences are highlighted with a red background; active sites are marked with blue pentagrams.

3.5. Expression and Purification of Recombinant BcPAD

SDS-PAGE analysis indicated that the molecular weight of recombinant BcPAD is 23.08 kDa (Figure 5), which is slightly higher than the 19.2 kDa reported for BsPAD-Q58 by Zhang et al [36]. This increase can be attributed to the fusion of a 33-amino acid histidine tag at the N-terminus of recombinant BcPAD, contributing an additional 3.45 kDa to its theoretical molecular weight. There was no significant difference in the expression levels of BcPAD induced by different IPTG concentrations (Figure 5A), and a large amount of target protein was produced after 3 h of induction at a lower IPTG concentration (final concentration of 0.1 mmol/L). Protein distribution analysis revealed that BcPAD mainly exists as a soluble protein at different induction temperatures (Figure 5B), and it was present in both the supernatant and precipitate when induced at 37 °C (Figure 5B). Previous studies have confirmed that low-temperature induction can reduce the rate of protein expression, facilitating proper protein folding and thereby increasing the yield of soluble proteins [37,38]. Consequently, induction at lower temperatures is more advantageous for the expression of soluble BcPAD. The soluble protein in the supernatant was purified using Ni-NTA affinity chromatography to obtain purified BcPAD (Figure 5C), with a protein concentration of 0.1354 mg/mL.

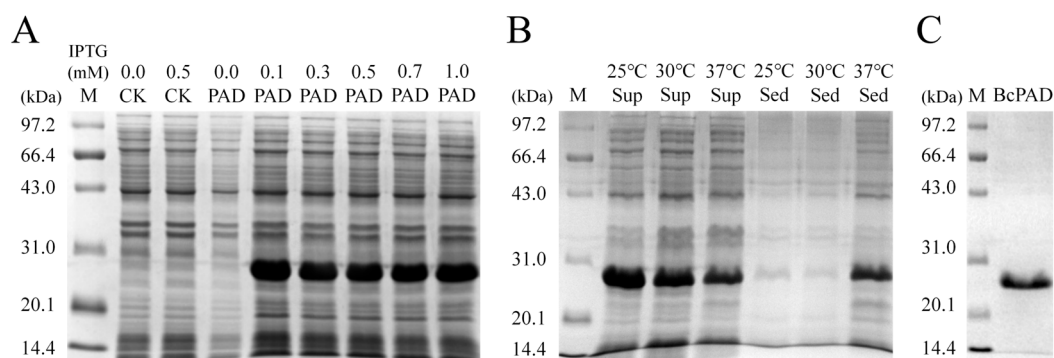


Figure 5. SDS-PAGE analysis of recombinant BcPAD. (A) Induction of recombinant BcPAD with different concentrations of IPTG. CK: *E. coli* BL21(DE3)-pET28a. (B) Induction of recombinant BcPAD at different temperatures. Sup: supernatant; Sed: precipitate. (C) Purification of recombinant BcPAD. M: protein molecular weight marker.

3.6. Effects of pH and Temperature on the Activity and Stability of BcPAD

BcPAD exhibits activity across a pH range of 5.0 to 8.0, with an optimal pH of 6.0 (Figure 6A), which is consistent with the optimal pH of LbPAD from *Lactobacillus brevis* [10] and is close to the 5.7 of AlPAD from *Aspergillus luchuensis* [39]. Although the activity of BcPAD significantly decreases under both acidic and alkaline conditions, it retains relative activities of 28.58% and 29.94% at pH 5.0 and pH 8.0, respectively, which differs from the result that LbPAD loses activity under pH 8.0 conditions [10]. After treatment for 5 h within the pH range of 5.0 to 6.0, the relative activity of BcPAD remains above 40% (Figure 6B). Under pH 8.0 conditions, enzyme activity is only about 20% after 5 h. These results suggest that a mildly acidic environment may be beneficial for the catalytic activity of BcPAD.

It has been reported that the structure and kinetics of enzymes may change with variations in temperature, thereby affecting their catalytic efficiency [40]. As shown in Figure 6C, BcPAD exhibits

activity across a temperature range of 20–70 °C, with an optimal reaction temperature of 50 °C, which is consistent with the findings reported by Ni et al. [41] and is higher than the optimal temperatures of 35 °C for LvPAD from *L. vermolensis* [2] and 37 °C for BIPAD from *B. licheniformis* [30]. In the temperature range of 30–40 °C, the relative enzyme activity gradually decreases with extended incubation time, but remains above 60% after 5 h. At the optimal temperature of 50 °C, the relative enzyme activity maintained 63% even after 4 h. When the temperature is raised to 70 °C, the relative activity remains at 16% for 2 h but is completely inactivated after 3 h. Overall, BcPAD exhibits a certain degree of thermal tolerance.

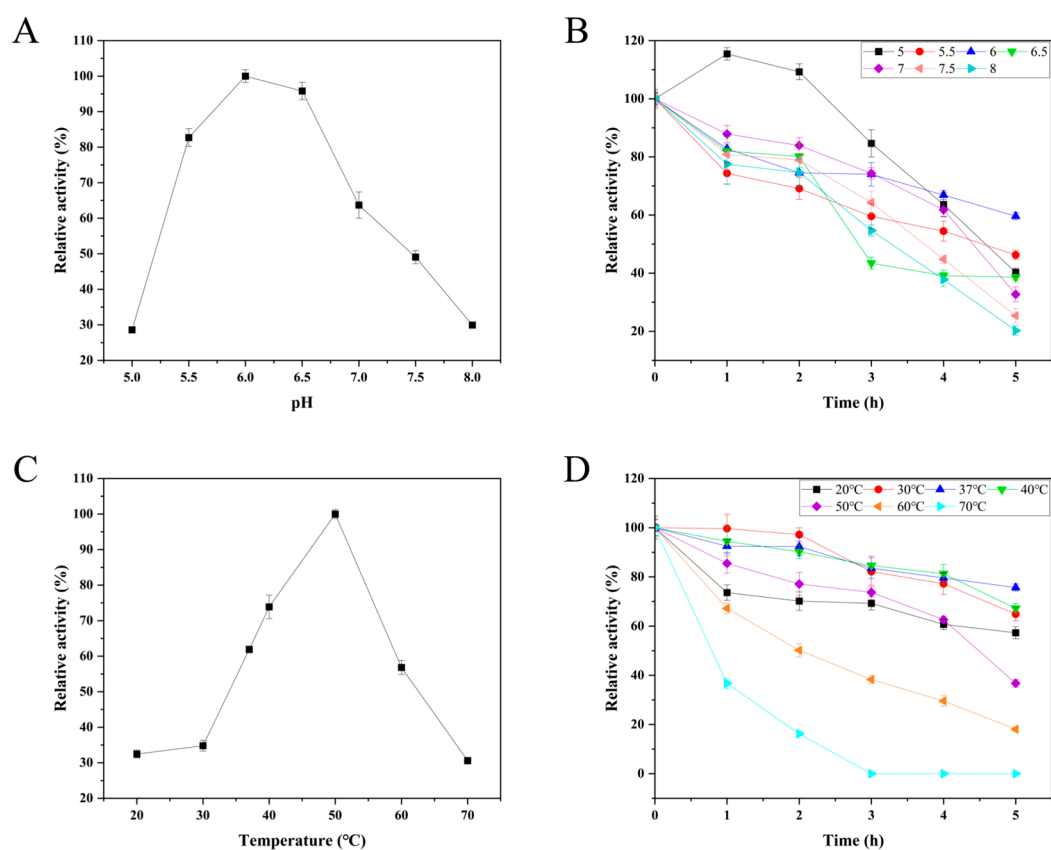


Figure 6. Enzymatic characteristics of BcPAD under different temperature and pH conditions. (A) Optimal pH of BcPAD. (B) pH stability of BcPAD. (C) Optimal temperature for BcPAD. (D) Temperature stability of BcPAD.

3.7. Effects of Metal Ions and Chemical Reagents on the Activity of BcPAD

The effects of metal ions and chemical reagents on BcPAD activity were evaluated using FA as the substrate (Figure 7). Ba^{2+} , Co^{2+} , Cu^{2+} , Mn^{2+} , and Zn^{2+} exhibited varying degrees of inhibition, with Zn^{2+} exerting the most pronounced inhibitory effect, reducing the relative activity of BcPAD by 34.92%. In contrast, Ca^{2+} , Fe^{3+} , Li^+ , and Mg^{2+} enhanced BcPAD activity, with Fe^{3+} being the most effective, increasing the relative activity to 115.36%. These metal ions were predominantly inhibitory in studies on LvPAD by Zhao et al. [2] and on BsPAD-Q58 by Zhang et al. [36], respectively, which may be attributable to the use of PCA as the substrate and differences in the sources of the phenolic acid decarboxylases. Triton X-100, ethanol, and EDTA exhibited no significant effect on BcPAD activity. However, SDS completely inactivated BcPAD, consistent with the findings for BaPAD reported by Li et al. [32]. Urea exhibited a moderate activating effect, increasing the relative activity to 109.49%, similar to the findings for LbPAD reported by Landete et al. [10].

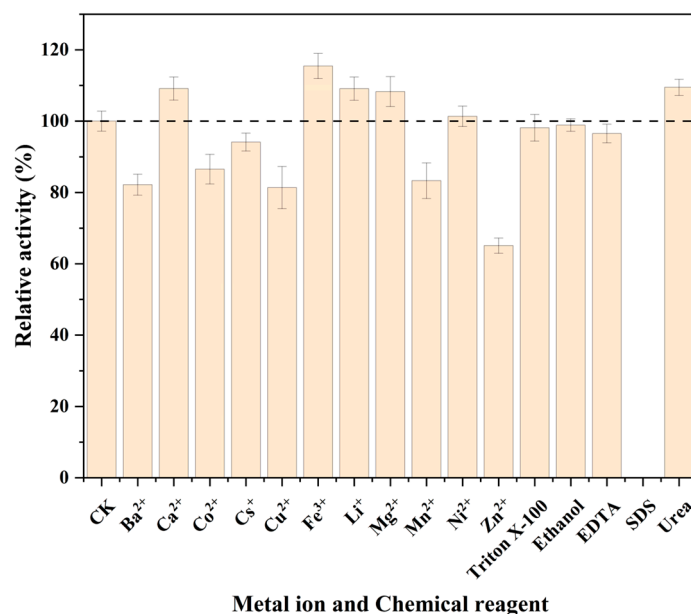


Figure 7. Effects of metal ions and chemical reagents on BcPAD activity.

3.8. Substrate Specificity and Kinetic Parameters of BcPAD

BcPAD exhibited significant substrate specificity and catalytic efficiency differences among various phenolic acid substrates. Substrate specificity analysis showed that BcPAD had the highest specific activity for PCA (460.55 ± 18.30 U/mg), identifying PCA as its preferred substrate (Table 3). The specific activity for CA was 145.88 ± 2.93 U/mg, lower than that for PCA, whereas that for FA was only 34.46 ± 1.11 U/mg. No enzymatic activity was detected for SA, suggesting that BcPAD scarcely catalyzes this substrate, consistent with previous report [10]. These results indicate that BcPAD has significant selectivity for structurally similar phenolic acids and prefers to catalyze the conversion of PCA.

Table 3. Substrate specificity of BcPAD.

Substrates	Specific activity (U/mg)	Relative activity (%)
Ferulic acid	34.46 ± 1.11	7.48
<i>p</i> -Coumaric acid	460.55 ± 18.30	100
Caffeic acid	145.88 ± 2.93	31.68
Sinapic acid	ND	ND

Different phenolic acids at a concentration of 80 mM were used as substrates for the assay, and all other assay conditions were identical. ND indicates that no activity was detected.

The kinetic parameters further supported this substrate preference (Table 4). PCA exhibited the highest V_{max} and K_{cat} values (837.06 ± 10.70 U/mg and 167.12 ± 2.14 s⁻¹, respectively), and the highest K_{cat}/K_m (6.26 ± 0.75 mM⁻¹ • s⁻¹), demonstrating that BcPAD achieves its highest overall catalytic efficiency with PCA at optimal substrate concentrations. In contrast, although FA had the lowest K_m value (4.72 ± 0.68 mM), reflecting the highest affinity for the enzyme, its V_{max} and K_{cat} were significantly lower (35.28 ± 0.61 U/mg and 7.04 ± 0.12 s⁻¹), resulting in a K_{cat}/K_m value of only 1.49 ± 0.22 mM⁻¹ • s⁻¹ and consequently lower overall catalytic efficiency. CA exhibited K_m , V_{max} , K_{cat} , and K_{cat}/K_m values that intermediate between those of PCA and FA. In summary, the combined substrate specificity and kinetic analyses demonstrated that BcPAD has a clear catalytic advantage for PCA, while its catalytic performance for FA and CA was comparatively weaker, similar to previous reports [42,43].

Table 4. Kinetic parameters of BcPAD.

Kinetic Parameters	Substrates		
	Ferulic acid	p-Coumaric acid	Caffeic acid
K_m (mM)	4.72 ± 0.68	26.70 ± 3.17	10.16 ± 1.36
V_{max} (U/mg)	35.28 ± 0.61	837.06 ± 10.70	155.99 ± 3.42
K_{cat} (s^{-1})	7.04 ± 0.12	167.12 ± 2.14	31.14 ± 0.68
K_{cat}/K_m ($mM^{-1} \cdot s^{-1}$)	1.49 ± 0.22	6.26 ± 0.75	3.06 ± 0.41

Kinetic analyses were conducted at pH 6.0 and 50 °C for 5 min using phenolic acids at concentrations ranging from 5.00 to 160.00 mM.

3.9. Structural Analysis of BcPAD

Homology modeling based on crystal structures is an effective approach for predicting protein tertiary structures, which is helpful for analyzing the molecular mechanisms of enzymatic property differences at the structural level [44]. The above results indicate that BcPAD exhibits significant differences in its ability to catalyze different phenolic acid substrates. To clarify the basis of these differences, homology modeling and molecular docking analyses were carried out. The results showed that BcPAD forms a dimer composed of two monomers (Figure 8A), consistent with the structure previously reported [34,45]. Ramachandran plot analysis revealed that over 97% of the residues of BcPAD are positioned within favored regions (Figure 8B), confirming the reliability of the model. Furthermore, the three-dimensional structure of BcPAD is highly similar to those of LpPDC (PDB ID: 2W2A) and BpPAD (PDB ID: 3NAD), with only minor differences at the N-terminus, C-terminus, and some random coil regions (Figure 8C). Previous studies have suggested that the N-terminus and C-terminus are closely associated with substrate specificity in phenolic acid decarboxylases [31,42,46].

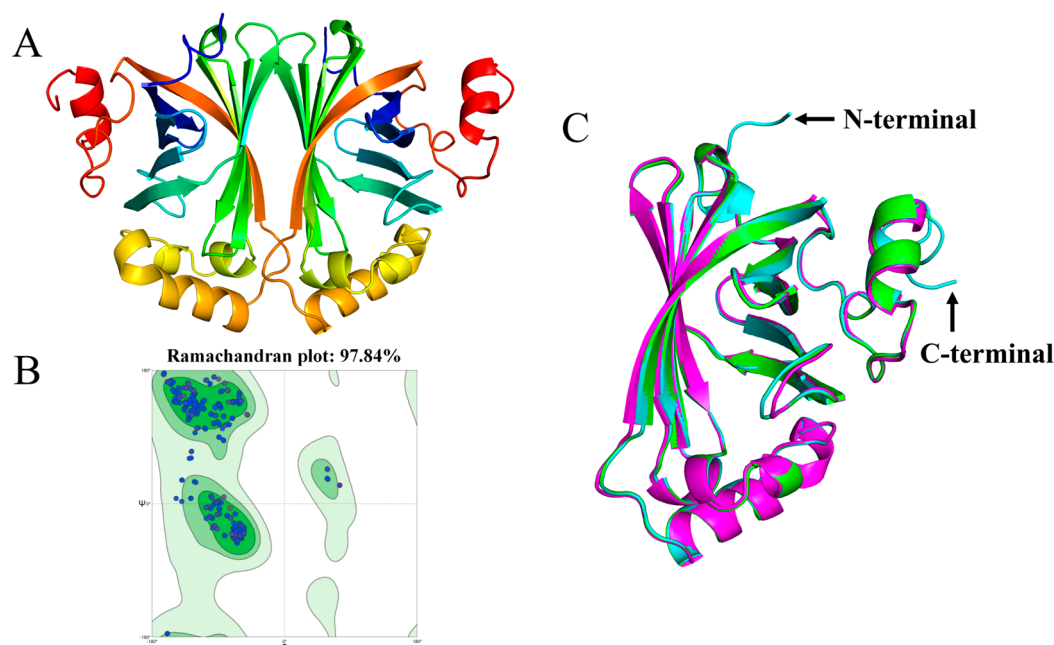


Figure 8. Three-dimensional structure and ramachandran plot assessment of BcPAD. (A) Three-dimensional structure of BcPAD. (B) Results of Ramachandran plot assessment. (C) Superposition of monomer structures, green represents BcPAD, blue represents LpPDC (PDB ID: 2W2A), and purple represents BpPAD (PDB ID: 3NAD).

To further investigate the structural basis for the differences in the catalytic performance of BcPAD toward various phenolic acid substrates, molecular docking analyses were performed to examine the binding modes of PCA, CA, and FA to BcPAD (Figure 9). The results showed that all

three substrates exhibited the same minimum binding energy (-6.8 kcal/mol), indicating similar overall binding affinities, although their binding modes and interaction patterns differed substantially. Among the three substrates, FA interacted with the largest number of residues, involving 18 amino acid residues (Figure 9A), including 11 van der Waals interactions, 2 carbon-hydrogen bonds, and 5 hydrophobic interactions, such as Pi-Pi T-shaped, Alkyl, and Pi-Alkyl (Figure 9D). These observations suggest that FA binds tightly within the active site primarily through nondirectional hydrophobic interactions and van der Waals forces but lacks specific hydrogen bonds with key polar or catalytic residues. Previous studies have shown that binding stability can be enhanced by hydrophobic interactions, hydrogen bonding, and electrostatic interactions [47,48]. The “multipoint hydrophobic restraint” mode of FA may therefore enhance binding stability while simultaneously limiting substrate conformational adjustment during catalysis, which is consistent with its kinetic profile of high affinity but low turnover and agrees with the findings of Zhou et al. [12].

By contrast, PCA interacted with 17 amino acid residues (Figure 9B), including 13 involved in van der Waals interactions, and formed two key hydrogen bonds with GLU-67 and THR-71, together with Pi-Alkyl hydrophobic interactions with VAL-73 and ILE-88 (Figure 9E). Previous studies have indicated that the hydrogen-bonding network formed by the substrate within the active site plays a crucial role in regioselectivity [49]. This binding mode not only ensures effective anchoring of the substrate within the active site but also facilitates the precise positioning of PCA in a conformation favorable for decarboxylation, thereby promoting transition-state formation and stabilization. This interpretation is consistent with the high V_{max} , K_{cat} , and K_{cat}/K_m values observed for PCA. CA displayed a binding pattern intermediate between those observed for FA and PCA. It interacted with 16 amino acid residues (Figure 9C), including 13 van der Waals interactions, and formed similar Pi-Alkyl hydrophobic interactions with VAL-73 and ILE-88; however, its hydrogen bonds were formed with TYR-14 rather than with GLU-67 and THR-71 (Figure 9F). This suggests that although CA can achieve relatively stable binding in the active site, the spatial orientation of its key functional groups is less optimally aligned with the catalytic residues than that of PCA, resulting in intermediate transition-state stability and catalytic efficiency.

Overall, differences in the catalytic performance of BcPAD toward different substrates are primarily determined by the hydrogen-bonding network, hydrophobic interactions, and the orientation and conformational compatibility of the substrates within the active site. Among these substrates, PCA adopts a more precise and catalytically favorable binding conformation, which provides an important structural basis for its recognition as the optimal substrate of BcPAD. These findings are consistent with previous reports [12,50].

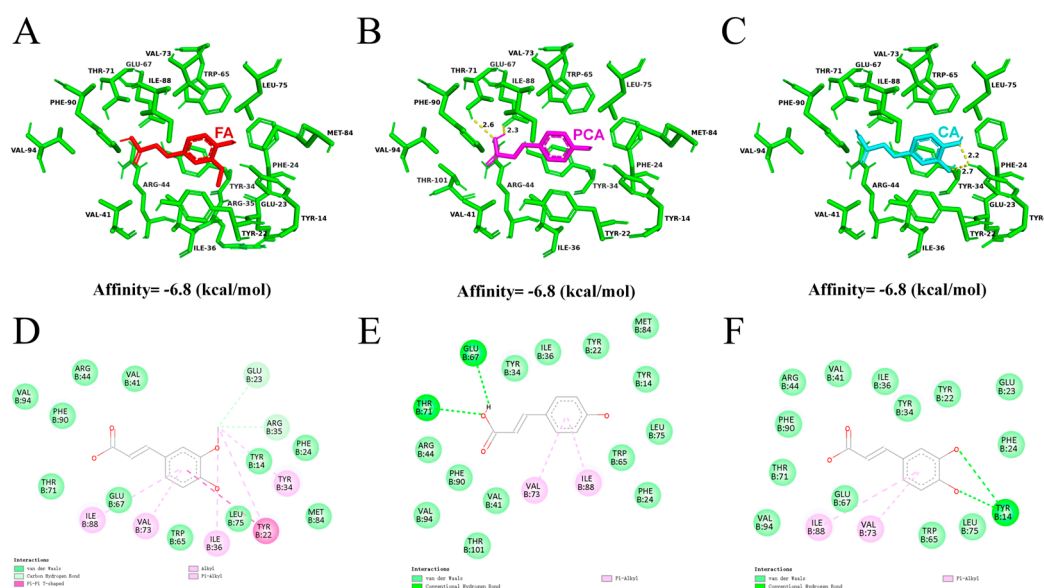


Figure 9. Molecular docking analysis of BcPAD with different phenolic acids. (A) Three-dimensional structure of BcPAD interacting with FA. (B) Three-dimensional structure of BcPAD interacting with PCA. (C) Three-dimensional structure of BcPAD interacting with CA. (D) Two-dimensional structure of BcPAD interacting with FA. (E) Two-dimensional structure of BcPAD interacting with PCA. (F) Two-dimensional structure of BcPAD interacting with CA.

4. Conclusions

In this study, *B. coagulans* JN11 was identified as the highest 4-EG-producing strain among the tested isolates, with a yield of 271.57 ± 2.73 $\mu\text{g/L}$. Its growth characteristics suggested adaptation to mildly acidic conditions and moderate temperatures. The phenolic acid decarboxylase gene, *BcPAD*, was successfully cloned from *B. coagulans* JN11 and heterologously expressed in *E. coli* BL21(DE3). Recombinant BcPAD showed optimal activity at pH 6.0 and 50 °C, retained considerable stability under mildly acidic conditions and at moderate temperatures, and responded differentially to metal ions and chemical reagents. Ca^{2+} , Fe^{3+} , Li^{+} , Mg^{2+} , and urea enhanced enzyme activity, whereas Zn^{2+} markedly inhibited enzyme activity and SDS completely inactivated the enzyme. Substrate specificity and kinetic analyses demonstrated that BcPAD preferentially catalyzed PCA, whereas CA and FA were converted less efficiently, and no activity was detected toward SA. Notably, although FA exhibited a lower K_m , its much lower turnover indicated that catalytic efficiency was not determined solely by substrate affinity. Structural modeling and molecular docking suggested that the superior catalytic performance toward PCA was associated with a more favorable binding orientation and productive hydrogen-bonding interactions with key active-site residues. Overall, these findings provide mechanistic insights into substrate recognition and catalysis by BcPAD and highlight the potential of *B. coagulans* JN11 and BcPAD in volatile phenol biosynthesis and flavor modulation during Baijiu production.

Author Contributions: Conceptualization, Y.L. and S.Y.; methodology, Y.L.; validation, Y.L., H.W., X.L., R.W., C.L., J.L., H.Z. and S.Y.; investigation, Y.L., H.W., X.L., R.W. and C.L.; resources, Y.L., J.L. and S.Y.; data curation, Y.L.; writing—original draft preparation, Y.L.; writing—review and editing, H.Z., J.L. and S.Y.; visualization, H.W. and X.L.; supervision, S.Y.; project administration, Y.L. All authors have read and agreed to the published version of the manuscript.

Funding: This work was funded by the Brewing Science and Technology Key Laboratory of Sichuan Province (NJ2024-PY-2) and the Undergraduate Innovation and Entrepreneurship Training Program of Sichuan University of Science & Engineering (CX2024133).

Institutional Review Board Statement: Not applicable.

Informed Consent Statement: Not applicable.

Data Availability Statement: The original contributions presented in the study are included in the article/Supplementary Material, further inquiries can be directed to the corresponding author.

Conflicts of Interest: The authors declare no conflicts of interest.

References

1. Zhang, Y.; Yu, X.; Zhao, X.; Liu, L.; Huang, Y.; Zhang, J.; Liu, J. Screening and identification of 4-ethylguaiacol-producing strain and its application in soy sauce brewing. *China Brewing* **2023**, *42*, 115-121.
2. Zhao, Y.; Zhu, B.; Zhou, Z.; Wu, Z.; Zhang, W. Cloning and characterization of phenolic acid decarboxylase responsible for aromatic volatile phenols production in Paocai based on metatranscriptomics. *Food Biosci.* **2023**, *55*, 102953.
3. Wang, C.; Li, L.; Fan, M.; Liu, J.; Yuan, S. Screening, identification and characterization of 4-ethylguaiacol producing *Bacillus* strains from jiangxiang *Daqu*. *Liquor-Making Science & Technology* **2023**, *346*, 45-52.

4. Zhao, D.; Shi, D.; Sun, J.; Li, H.; Zhao, M.; Sun, B. Quantification and cytoprotection by vanillin, 4-methylguaiacol and 4-ethylguaiacol against AAPH-induced abnormal oxidative stress in HepG2 cells. *Rsc Adv.* **2018**, *8*, 35474-35484.
5. Zhao, D.; Jiang, Y.; Sun, J.; Li, H.; Luo, X.; Zhao, M. Anti-inflammatory mechanism involved in 4-ethylguaiacol-mediated inhibition of LPS-induced inflammation in THP-1 cells. *J. Agric. Food. Chem.* **2019**, *67*, 1230-1243.
6. Weng, W.; Kuo, P.; Scofield, B.A.; Paraiso, H.C.; Brown, D.A.; Yu, I.; Yen, J. 4-Ethylguaiacol modulates neuroinflammation and promotes heme oxygenase-1 expression to ameliorate brain injury in ischemic stroke. *Front. Immunol.* **2022**, *13*, 887000.
7. Wang, Z.; Wang, S.; Liao, P.; Chen, L.; Sun, J.; Sun, B.; Zhao, D.; Wang, B.; Li, H. HS-SPME combined with GC-MS/O to analyze the flavor of strong aroma Baijiu *Daqu*. *Foods* **2022**, *11*, 116.
8. Wang, S.; Cao, R.; Shen, F.; Xiang, X.; Yan, S. Screening and identification of a 4-ethyl guaiacol-producing strain from nongxiang *Daqu*. *Liquor-Making Science & Technology* **2018**, *287*, 48-52.
9. Hou, R.; Wang, Y.; Yang, J.; Wei, H.; Yang, F.; Jin, Z.; Hu, J.; Gao, M. Bioconversion of waste generated during ethanol production into value-added products for sustainable utilization of rice straw. *Biochem. Eng. J.* **2020**, *164*, 107761.
10. Landete, J.M.; Rodríguez, H.; Curiel, J.A.; de Las Rivas, B.; Mancheño, J.M.; Muñoz, R. Gene cloning, expression, and characterization of phenolic acid decarboxylase from *Lactobacillus brevis* RM84. *J. Ind. Microbiol. Biotechnol.* **2010**, *37*, 617-624.
11. Tang, X.; Wu, S.; Hua, X.; Fan, Y.; Li, X. Ferulic acid triggering a co-production of 4-vinyl guaiacol and fumaric acid from lignocellulose-based carbon source by *Rhizopus oryzae*. *Food Chem.* **2024**, *461*, 140799.
12. Zhou, W.; Zhang, Q.; Huang, K.; Huang, Z.; Ding, W.; Sun, J.; Bai, W. Accelerating the conversion of black chokeberry anthocyanins toward vinylphenolic pyranoanthocyanins by displaying phenolic acid decarboxylase from *Lactiplantibacillus plantarum* on the surface of *Pichia pastoris*. *Food Chem.* **2025**, *476*, 143408.
13. Mathew, S.; Abraham, T.E. Bioconversions of ferulic acid, an hydroxycinnamic acid. *Crit. Rev. Microbiol.* **2006**, *32*, 115-125.
14. Chen, Y.; Qin, C.; Li, Q.; Hu, K.; Li, J.; Liu, S. Research progress in phenolic acid decarboxylase derived from microorganisms. *Food Science* **2024**, *45*, 323-332.
15. Gu, W.; Li, X.; Huang, J.; Duan, Y.; Meng, Z.; Zhang, K.; Yang, J. Cloning, sequencing, and overexpression in *Escherichia coli* of the *Enterobacter* sp. Px6-4 gene for ferulic acid decarboxylase. *Appl. Microbiol. Biotechnol.* **2011**, *89*, 1797-1805.
16. Cavin, J.F.; Dartois, V.; Diviès, C. Gene cloning, transcriptional analysis, purification, and characterization of phenolic acid decarboxylase from *Bacillus subtilis*. *Appl. Environ. Microbiol.* **1998**, *64*, 1466-1471.
17. Huang, H.; Tokashiki, M.; Maeno, S.; Onaga, S.; Taira, T.; Ito, S. Purification and properties of phenolic acid decarboxylase from *Candida guilliermondii*. *J. Ind. Microbiol. Biotechnol.* **2012**, *39*, 55-62.
18. Sheng, X.; Lind, M.E.S.; Himo, F. Theoretical study of the reaction mechanism of phenolic acid decarboxylase. *The Febs Journal* **2015**, *282*, 4703-4713.
19. Lu, C.; Zhang, J.; Zhao, X.; Zi, Y.; Xiao, X. Biotransformation of phenolic acids in foods: pathways, key enzymes, and technological applications. *Foods* **2025**, *14*, 2187.
20. Mu, Y.; Huang, J.; Zhou, R.; Mao, F.; Pan, Q.; Chen, S.; Lu, Z.; Du, L.; Xie, F. Exploring the response patterns of strong-flavor baijiu brewing microecosystem to fortified *Daqu* under different pit ages. *Food Res. Int.* **2022**, *155*, 111062.
21. Li, H.; Liu, S.; Liu, Y.; Hui, M.; Pan, C. Functional microorganisms in baijiu *Daqu*: research progress and fortification strategy for application. *Front. Microbiol.* **2023**, *14*, 1119675.
22. Szambelan, K.; Jeleń, H.; Nowak, J.; Frankowski, J.; Szwengiel, A. The promising prospective technology for biofuel production with mixed cultures using *Sorghum* grain (*Sorghum bicolor* (L.) Moench) grown in a temperate climate: characteristics of fermentation factors and volatile compounds analysis. *J. Agric. Food. Chem.* **2025**, *73*, 14408-14419.

23. Zhang, Y.; Sun, Q.; Liu, X.; Basit, R.A.; Ma, J.; Fu, Z.; Cheng, L.; Fan, G.; Teng, C. Screening, identification, and fermentation condition optimization of a high-yield 3-methylthiopropanol yeast and its aroma-producing characteristics. *Foods* **2024**, *13*, 418.
24. Kumar, A.; Singh, R.; Yadav, A.; Giri, D.D.; Singh, P.K.; Pandey, K.D. Isolation and characterization of bacterial endophytes of *Curcuma longa* L. *3 Biotech* **2016**, *6*, 60.
25. Zhang, Y.; Feng, Z.; Xiang, H.; Zhang, X.; Yang, L. Characterization of feruloyl esterase from *Klebsiella oxytoca* Z28 and its application in the release of ferulic acid from de-starching wheat bran. *Microorganisms* **2023**, *11*, 989.
26. Noskova, Y.; Pentekhina, I.; Seitkalieva, A.; Nedashkovskaya, O.; Goroshkova, Y.; Balabanova, L. Characterization of an atypical GH19 family chitinase from *Vibrio jasicida* KMM 6832. *Microorganisms* **2026**, *14*, 443.
27. Ma, Y.; Liu, L.; Hu, G.; Wang, S.; Shan, L.; Chen, J. Effect of non-*Saccharomyces* yeasts derived from traditional fermented foods on beer fermentation characteristics and flavor profiles. *Foods* **2025**, *14*, 1395.
28. Wang, M.; Zheng, X.; Bian, X.; Ren, J.; Bai, L.; Yao, Y.; Dong, B.; Zhao, G. *Bacillus licheniformis* and *Wickerhamiella versatilis*: sources of the pleasant smoky and fruity flavors of soybean paste. *Food Chem.* **2025**, *477*, 143218.
29. Suezawa, Y.; Suzuki, M. Bioconversion of ferulic acid to 4-vinylguaiacol and 4-ethylguaiacol and of 4-vinylguaiacol to 4-ethylguaiacol by halotolerant yeasts belonging to the genus *Candida*. *Biosci Biotech Bioch* **2007**, *71*, 1058-1062.
30. Hu, H.; Li, L.; Ding, S. An organic solvent-tolerant phenolic acid decarboxylase from *Bacillus licheniformis* for the efficient bioconversion of hydroxycinnamic acids to vinyl phenol derivatives. *Appl. Microbiol. Biotechnol.* **2015**, *99*, 5071-5081.
31. Frank, A.; Eborall, W.; Hyde, R.; Hart, S.; Turkenburg, J.P.; Grogan, G. Mutational analysis of phenolic acid decarboxylase from *Bacillus subtilis* (BsPAD), which converts bio-derived phenolic acids to styrene derivatives. *Catal. Sci. Technol.* **2012**, *2*, 1568-1574.
32. Li, L.; Long, L.; Ding, S. Bioproduction of high-concentration 4-vinylguaiacol using whole-cell catalysis harboring an organic solvent-tolerant phenolic acid decarboxylase from *Bacillus atrophaeus*. *Front. Microbiol.* **2019**, *10*, 1798.
33. Matte, A.; Grosse, S.; Bergeron, H.; Abokitse, K.; Lau, P.C.K. Structural analysis of *Bacillus pumilus* phenolic acid decarboxylase, a lipocalin-fold enzyme. *Acta Crystallographica Section F* **2010**, *66*, 1407-1414.
34. Rodríguez, H.; Angulo, I.; de Las Rivas, B.; Campillo, N.; Páez, J.A.; Muñoz, R.; Mancheño, J.M. *p*-Coumaric acid decarboxylase from *Lactobacillus plantarum*: structural insights into the active site and decarboxylation catalytic mechanism. *Proteins: Structure, Function, and Bioinformatics* **2010**, *78*, 1662-1676.
35. Myrtollari, K.; Calderini, E.; Kracher, D.; Schöngaßner, T.; Galušić, S.; Slavica, A.; Taden, A.; Mokos, D.; Schrifer, A.; Wirnsberger, G.; Gruber, K.; Daniel, B.; Kourist, R. Stability increase of phenolic acid decarboxylase by a combination of protein and solvent engineering unlocks applications at elevated temperatures. *ACS Sustain. Chem. Eng.* **2024**, *12*, 3575-3584.
36. Zhang, L.; Shen, J.; Ren, M.; Xu, Y.; Lin, S.; Bao, S.; Wang, L.; Fan, R.; Jin, L.; Quan, C. Characterization and modification of phenolic acid decarboxylase from marine bacteria for the synthesis of 4-vinyl phenol derivatives. *BMC Microbiol.* **2025**, *26*, 31.
37. Liu, Y.; Liu, L.; Yang, S.; Liu, G.; Zeng, Q.; Liu, Y. Molecular characterization and functional analysis of a pathogenesis-related β -1,3-glucanase gene in spruce (*Picea asperata*). *Eur. J. Plant Pathol.* **2022**, *164*, 177-192.
38. Liu, Y.; Liu, L.; Yang, C.; Han, S.; Yang, S.; Liu, G.; Zeng, Q.; Liu, Y. Molecular identification and antifungal activity of a defensin (PaDef) from spruce. *J. Plant Growth Regul.* **2022**, *41*, 494-506.
39. Maeda, M.; Tokashiki, M.; Tokashiki, M.; Uechi, K.; Ito, S.; Taira, T. Characterization and induction of phenolic acid decarboxylase from *Aspergillus luchuensis*. *J. Biosci. Bioeng.* **2018**, *126*, 162-168.
40. Arcus, V.L.; van der Kamp, M.W.; Pudney, C.R.; Mulholland, A.J. Enzyme evolution and the temperature dependence of enzyme catalysis. *Curr. Opin. Struct. Biol.* **2020**, *65*, 96-101.
41. Ni, J.; Wu, Y.; Tao, F.; Peng, Y.; Xu, P. A coenzyme-free biocatalyst for the value-added utilization of lignin-derived aromatics. *J. Am. Chem. Soc.* **2018**, *140*, 16001-16005.

42. Li, Q.; Xia, Y.; Zhao, T.; Gong, Y.; Fang, S.; Chen, M. Improving the catalytic characteristics of phenolic acid decarboxylase from *Bacillus amyloliquefaciens* by the engineering of N-terminus and C-terminus. *BMC Biotechnol.* **2021**, *21*, 44.
43. Maeda, M.; Motosoko, M.; Tokashiki, T.; Tokashiki, J.; Mizutani, O.; Uechi, K.; Goto, M.; Taira, T. Phenolic acid decarboxylase of *Aspergillus luchuensis* plays a crucial role in 4-vinylguaiaicol production during awamori brewing. *J. Biosci. Bioeng.* **2020**, *130*, 352-359.
44. Liu, Y.; Zhang, X.; Yuan, S.; Liu, J. Molecular identification and functional characterization of a chitinase gene in *Picea asperata*. *Discover Plants* **2025**, *2*, 145.
45. Godoy, L.; Martínez, C.; Carrasco, N.; Ganga, M.A. Purification and characterization of a *p*-coumarate decarboxylase and a vinylphenol reductase from *Brettanomyces bruxellensis*. *Int. J. Food Microbiol.* **2008**, *127*, 6-11.
46. Gu, W.; Yang, J.; Lou, Z.; Liang, L.; Sun, Y.; Huang, J.; Li, X.; Cao, Y.; Meng, Z.; Zhang, K. Structural basis of enzymatic activity for the ferulic acid decarboxylase (FADase) from *Enterobacter* sp. Px6-4. *Plos One* **2011**, *6*, e16262.
47. Mphahlele, M.J.; Magwaza, N.M.; Gildenhuis, S.; Setshedi, I.B. Synthesis, α -glucosidase inhibition and antioxidant activity of the 7-carbo-substituted 5-bromo-3-methylindazoles. *Bioorganic Chem.* **2020**, *97*, 103702.
48. Yang, D.; Chen, X.; Liu, X.; Han, N.; Liu, Z.; Li, S.; Zhai, J.; Yin, J. Antioxidant and α -glucosidase inhibitory activities guided isolation and identification of components from mango seed kernel. *Oxidative Med. Cell. Longev.* **2020**, *2020*, 8858578.
49. Chen, T.; Chen, Z.; Wang, N.; Chu, J.; Fan, B.; Cheng, C.; Qin, S.; He, B. Highly regioselective and efficient biosynthesis of polydatin by an engineered UGTBL1-AtSuSy cascade reaction. *J. Agric. Food. Chem.* **2021**, *69*, 8695-8702.
50. Parada-Fabián, J.C.; Hernández-Sánchez, H.; Méndez-Tenorio, A. Substrate specificity of the phenolic acid decarboxylase from *Lactobacillus plantarum* and related bacteria analyzed by molecular dynamics and docking. *J. Plant Biochem. Biotechnol.* **2019**, *28*, 91-104.

Disclaimer/Publisher's Note: The statements, opinions and data contained in all publications are solely those of the individual author(s) and contributor(s) and not of MDPI and/or the editor(s). MDPI and/or the editor(s) disclaim responsibility for any injury to people or property resulting from any ideas, methods, instructions or products referred to in the content.